CHAPTER 4

FUNDAMENTAL OF GAS-LIQUID-SOLID FLUIDIZATION

The expression of three-phase fluidization was used to discribe fluidizaton of solid particles by two fluids. A gas and a liquid were the fluidizing media used in the applications. Studies of three-phase fluidization had been of interest and their numerous applications existed in various industrial processes, which varied in size from bench to commercial scale. In such system, the individual phases could be reactants, products, catalysts, or inert. Some examples of three-phase fluidization applications were shown in Table 4-1.

In general, a gas-liquid-solid fluidized bed, a continuous liquid phase would flow upwards while gas phase was in discrete bubbles flowing cocurrently. To apply gas-liquid-solid fluidization system for microalgae cells, it was necessary to understand the phenomena, as well as influences of, the parameters of such fluidized bed on the cell disruption.

Table 4-1. Examples of applications of three-phase fluidized bed processing.

Physical processing	Chemical processing	Biochemical processing
Drying of calcium carbonate and polyvinylchloride	Production of zinc hydrosulfite	Aerobic biological waste treatment
Dust collection	Methanol fermentation	Production of animal cells
Crystallization	Electrode	Enzyme immobilization
Sand filter cleaning	Coal liquefaction	Ethanol fermentation
Drying of granular material	Coal gasification	Antibiotic production
Lactose granulation	Fuel gas desulfurization	Conversing of sucrose to glucose by plant cells

4.1 Gas-Liquid-Solid Fluidization

As mentioned previously, the gas-liquid-solid fluidization was an operation, in which the solid particles layer, fluidized by gas and liquid and then behaved like a fluid. In general, the state of the particle motion in the fluidized bed operation by the upward flow of the fluid could be subdivided into three basic operating regimes: the fixed bed regime, the expanded bed regime, and the transport regime.

The fixed bed regime existed when the drag force on the particle induced by the flow of a gas-liquid mixture was smaller than the effective weight of the particle layer. With an increase in gas and/or liquid velocity, the drag force counterbalances the effective weight of the particles then the bed would achieve the state of minimum fluidization and marked the onset of the expanded bed regime. With a further increase in gas and/or liquid velocity beyond the minimum fluidization velocity, the solid bed would change to the expanded bed regime until the gas or liquid velocity reached the terminal velocity of the particles in the medium (U_t'). At the gas or liquid velocity above U_t', operation would be considered as the transport regime.

4.2 Hydrodynamics

Hydrodynamic behavior of three-phase fluidized bed reflected the complex interactions between the individual phases. The most prominent interaction occurred between the rising gas bubbles and the surrounding liquid-solid mixture. Three distinct regions above the gas-liquid distributor were identifiable based on the prevailing physical phenomena: the distributor region, the bulk fluidized bed region, and the free board region. A schematic diagram was shown in Figure 4-1.

The distributor region referred to the region immediately above the gas-liquid distributor where gas spouts might occur. It included the region from initial bubble formation to the establishment of the final bubble shape. The hydrodynamic behavior in the distributor region inherently depended on the gas-liquid distributor design and the physical properties of the liquid-solid medium.

The bulk fluidized bed region included the main portion of the fluidized bed. The hydrodynamic behavior in the bulk fluidized bed region varied drastically over large ranges of operating conditions. However, for a given operating condition, there was a minimum axial transport property variation in the region.

Drastically different from the previous regions, the freeboard region mainly contained entrained particles from the bulk fluidized bed region. Particle entrainment led to a solids hold up profile above the fluidized bed surface that decreased axially in a manner similar to that in a gas-solid fluidized bed. Generally, the demarcation between the freeboard region and the bulk fluidized bed region was much more distinct for large/heavy particles than for small/light particles.

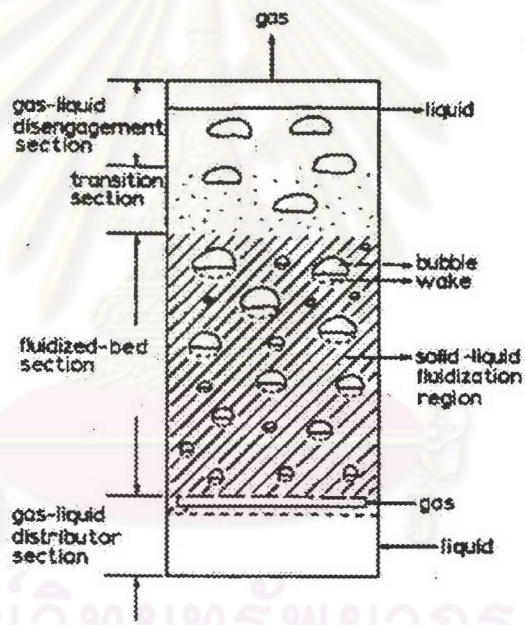

Figure 4-1. Schematic representation of gas-liquid-solid fluidized bed for cocurrent upward gas-liquid-solid systems with liquid as the continuous phase. (Redrawn from Muroyama and Fan. AIChE J. 1985, 31, 1, p.7)

4.2.1. Pressure Drop and Phase Holdup

When consider a fluidized bed column, which was partly filled with a fine granular material as shown schematically in Figure 4-2. The column was opened at the top and had a porous plate at the bottom to support the bed and to distribute the flow

uniformly over the entire cross section. Fluid was admitted below the distributor plate at a low flow rate and passes upward through the bed without causing any particle motion. If the particles were quite small, flow in the channels between the particles would be laminar and the pressure drop across the bed would be proportional to the superficial velocity. As the fluid velocity was gradually increased, the pressure drop increased, but the particles did not move and the bed height remained the same. At a certain velocity, the pressure drop across the bed counterbalances the force of gravity on the particles or the weight of the bed, and any further increase in velocity caused the particles to move. This was point A on the graph. Sometimes the bed expanded slightly with the grains still in contact, since just a slight increased in porosity, ε could offset an increase of several percent in superficial constant and keep pressure drop, ΔP constant. With a further increase in velocity, the particles became separated enough to move above in the bed, and true fluidization begins (point B).

Once the bed was fluidized, the pressure drop across the bed became constant, but the bed height continues to increase with increasing flow. The bed could be operated at quite high velocities with very little or no loss of solids, since the superficial velocity needed to support a bed of particle was much less than the terminal velocity for individual particles.

If the flow rate to the fluidized bed was gradually reduced, the pressure drop remained constant, and the bed height decreased, following the line BC that was observed for increasing velocities. However, the final bed height might be greater than the initial value for the fixed bed, since solids dumped in a column tended to pack more tightly than solids slowly settling from a fluidized bed state. The pressure drop at low velocities was then less than in the original fixed bed. On starting up again, the pressure drop offset the weight of the bed at point B, and this point, rather than point A, should be considered to give the minimum fluidization velocity, u_{mf}. To measure u_{mf}, the bed should be fluidized vigorously, allowed to settle with the fluid turn off, and the flow rate increased gradually until the bed starts to expand. More reproducible value of u_{mf} could sometimes be obtained from the intersection of the graphs of pressure drop in the fixed bed and the fluidized bed.

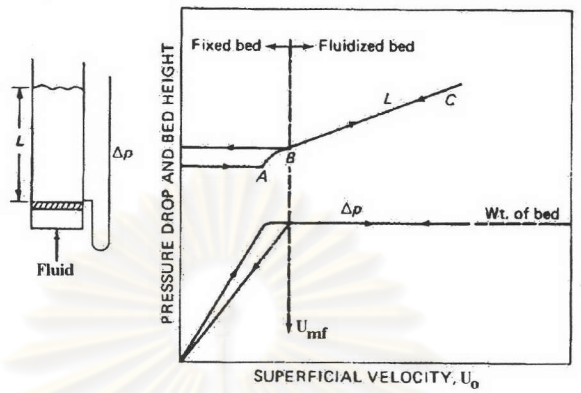

Figure 4-2. Pressure drop and bed height and superficial velocity for a bed of solid. (Redrawn from McCabe et al, Unit operation of chemical engineering. 1993, p.165)

The pressure drop through the bed was strongly related to the individual phase holdup in the bed. The phase holdup was defined as the fraction of the solids, liquid or gas phase to volume of the column. In the fluidized bed section with low solids entrainment rates, the solid holdup, ε_s, could be expressed as

$$\varepsilon_s = \frac{w}{\rho_s SH} \qquad (4\text{-}1)$$

However, behavior of gas holdup in the freeboard region strongly depended on the flow regimes and hence, on both particle and liquid properties. Gas holdup in three-phase fluidized beds could be lower than that in a corresponding bubble column because the particles promoted bubble coalescence, however it could also be higher than that in a corresponding bubble column when the particles helped break up gas bubble in some certain operating ranges. Furthermore, gas holdup was important for determining residence time of the gas in liquid. Kato et al. (1985) had proposed that the

gas holdup in a system of gas-liquid-solid fluidization could be approximated by the following equation;

$$\varepsilon_g = 0.3\, W^{1.3}/(1 + 1.1W^{1.15}) \quad (4\text{-}2)$$

when the parameter W was defined as

$$W = (gD_c^2\rho_l/\sigma)^{0.198}(gD_c^3/\nu_l^2)^{0.035}(U_g/\sqrt{gD_c} \quad (4\text{-}3)$$

The following relationship held among individual holdups:

$$\varepsilon_g + \varepsilon_l + \varepsilon_s = 1 \quad (4\text{-}4)$$

Under the steady state condition, the total axial pressure gradient (static pressure gradient) at any cross section in the column represented the total weight of the bed consisting of the three phases per volume as given by

$$-\frac{dP}{dz} = (\varepsilon_g\rho_g + \varepsilon_l\rho_l + \varepsilon_s\rho_s)g \quad (4\text{-}5)$$

where $\varepsilon_g, \varepsilon_l, \varepsilon_s$ = gas, liquid, and solid holdup (-), respectively.

ρ_g, ρ_l, ρ_s = gas, liquid, and solid density (kg/m^3), respectively.

w = weight of solid particle in the bed (kg).

S = cross-section area of empty column (m).

H = effective height of bed expansion (m).

g = gravitational acceleration (m/s^2).

dP/dz = static pressure gradient.

D_c = column diameter (m)

ρ_l = liquid density (kg/m^3)

σ = surface tension (mN/m)

ν_l = kinematic liquid viscosity (m^2/s)

U_g = gas velocity

The frictional drag on the wall of the column and the acceleration of the gas and liquid flows could be neglected. In equation (4-3), the term $\varepsilon_g \rho_g$ in the right hand side was usually negligibly small compared to the other terms. The evaluation of individual phase holdups based on the pressure gradient method, ε_s could be directly obtained from equation (4-1) with the height of bed expansion measured experimentally while ε_g could be directly calculated from equation (4-2). Finally, ε_l could be calculated from equation (4-4) and (4-5) simultaneously with the experimentally measured static pressure gradient.

4.2.2. Flow Regime

Three flow regimes could be identified based on the bubble flow behavior in three-phase fluidized bed: the coalesced bubble, the dispersed bubble, and the slugging regimes. In the coalesced bubble regime, bubbles tended to coalesce and both the bubble size and velocity became large and shown a wide distribution. Colesced bubbles rose near the column near the column center with high velocity and stirred the bed violently. The coalesced bubble regime predominated at low liquid and high gas velocities. In the dispersed bubble regime, no bubble coalescence occurred and the bubbles were of uniform, small size. The dispersed bubble regime predominated at high liquid velocities and at low and intermediate gas velocities. In a small diameter column (e.g., D_c < 15 cm), the gas bubble could easily grew to the size of the column diameter at high gas flow rates creating "slug" bubbles which occupied nearly the whole cross section. In columns of large diameter, however, slugging might not occur. The flow regimes varied significantly with the column diameter. Particle properties also profoundly affected the prevailing flow regime at given gas and liquid velocities and terminal velocity of the fluidized particles affected the liquid velocity of transition from the coalesced to the dispersed bubble regime

4.3 Agitation

In this experiment, agitator was used to increaseing efficiency of microorganism disruption. Details of those were as follows;

4.3.1 Classification of Agitators

Agitators were divided into two classes: those that generate currents parallel with the axis of the agitator shaft and those that generated currents in a tangential or radial direction. The first were called axial-flow agitators, the second radial-flow agitators.

The three main type of agitator were propeller, paddle, and turbine. Some of them were shown in Figure 4-3

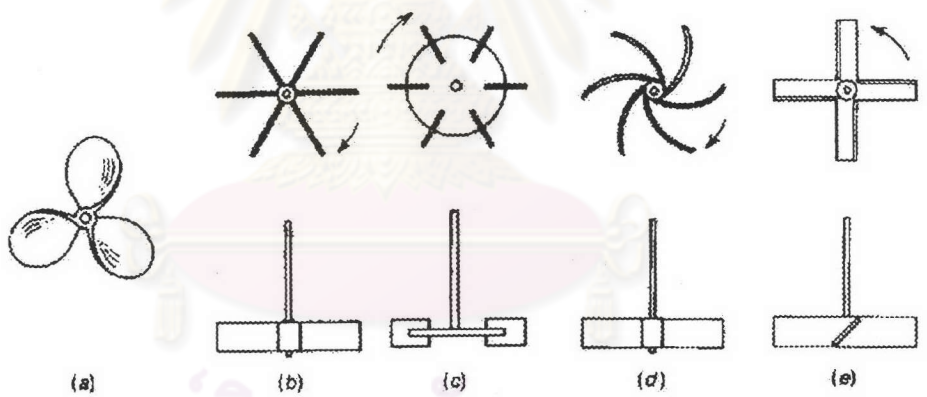

Figure 4-3. Some of many design of mixing agitator (a) three-blade marine propeller; (b) open straight-blade turbine; (c) bladed disk turbine; (d) vertical curved-blade turbine; (e) pitched-blade turbine (Redrawn from McCabe et al, Unit operation of chemical engineering. 1993, p.238)

1. Propellers

A propeller was an axial-flow, high-speed agitator for liquids of low viscosity. The flow currents leaving the agitator continued through the liquid in a given direction until deflected by the wall or the floor of the column. The highly turbulent

swirling column of liquid leaving the agitator entrained stagnant liquid as it moves along. The propeller blades vigorously cut or sheared the liquid. Because of the persistence of the flow currents, propeller agitators were effective in very large vessels. In a deep tank two or more propellers might be mounted on the same shaft, usually direction the liquid in the same directions, or in the same direction. Sometime two propellers worked in opposite directions, or in "push-pull," to create a zone of especially high turbulence between them.

2. Paddles.

Paddles turned at slow to moderate speeds in the center of a column. They pushed the liquid radially and tangentially with almost no vertical motion at the agitator unless the blades were pitched. The current they generated travel outward to the column wall and then either upward or downward.

3. Turbine

Some of the many designs of turbine were shown in Fig 4-3 b, c, d, and e. Most of turbines resembled multi-bladed paddle agitators with short blades as turning at high speed on a shaft mounted centrally in the column. The blades might have straight or curved, pitched or vertical. Turbines were effective over a very wide range of viscosity. In low viscosity liquid turbines generated strong currents that persisted throughout the column, seeking out and destroying stagnant pockets. Near the agitator was a zone of rapid currents, high turbulence, and intense shear. The principle currents were radial and tangential. The tangential components induced vortexing and swirling, which must be stopped by baffles or by a diffuser ring if the agitator was to be most effective.

Because the results in this experiment required, fluidization must have enough power for cell disruption. Thereby turbines were used for piercing of liquid in column. Finally solid phase would collide with themselfand turbulence flow would happen.

4.3.2 Flow Patterns in Agitated Column

In general case, type of flow on an agitated column depended on the type of agitator; the characteristics of the fluid; and the size and proportion of tank, baffles, and agitator. The velocity of the fluid at any point in the tank had three companents, and the overall flow pattern in the tank depended on the variations in these three-velocity components from point to points. The first velocity component was radial and acts in a direction perpendicular to the shaft of the agitator. The second component was longitudinal and acts in a direction parallel with the shaft. The third component was tangential, or rotational, and acts in a direction tangent to a circular path around the shaft. In the usually case, the shaft was vertical and centrally located in the column, the radial and tangential components were in a horizontal plane and the longitudinal component was vertical. The radial and longitudinal components were useful and provide the flow necessary, while the component was generally disadvantageous due to the tangential flow follows a circular path around the shaft and creates a vortex in the liquid, as shown in Figure 4-4. If solid particles were present, circulatory currents tended to throw the particles to the outside by centrifugal force, from where they moved downward and to the center of the tank at the bottom. Instead of mixing, its reverse, the solid concentration occurred at the side of the bottom of the column. In unbaffled column, circulatory flow occurred by all types of agitators, whether axial flow or radial flow. If the swirling was storng, the flow pattern in the column was virtually the same regardless of the design of the agitator. At high agitator speeds the vortex might be so deep that it reached the agitators, and gas from above the liquid was drawn down into charge. Generally this was undesirable.

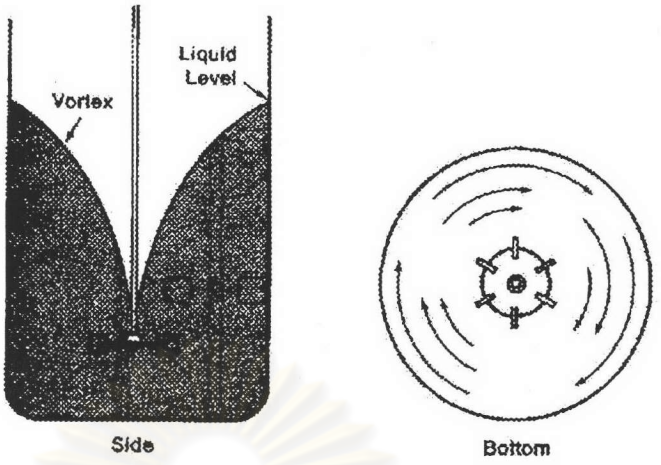

Figure 4-4. Flow pattern of a radial-flow turbine in an unbaffled column (Redrawn from McCabe et al, Unit operation of chemical engineering. 1993, p.239)

In this study, draft tube was used in the system for improve efficiency of fluidization.

4.3.3 Draft Tube

There was return flows to an agitator of any type of agitator from all directions, because it was not under the control of solid surfaces. In most applications of agitator mixers this was not a limitation, but when the direction and velocity of flow to the suction of the agitator were to be controlled, draft tubes were used, as shown in Fig. 4.5. These devices might be useful when high shear at the agitator itself was desired, as in the manufacture of certain emulsions, or where solid particles that tended to float on the surface of the liquid in the tank were to be dispersed in the liquid. Draft tubes could add the fluid friction in the system, and for a given power input, they reduced the rate of flow so that they were not used unless they were required.

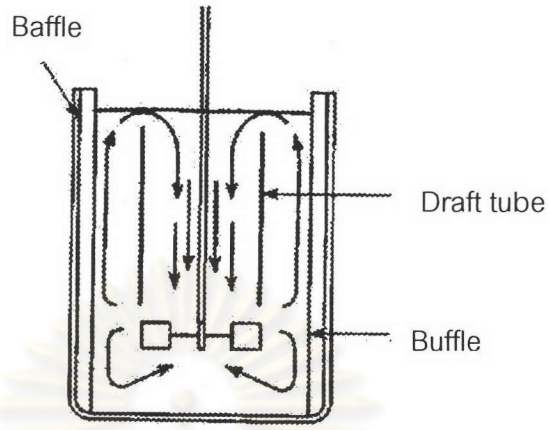

Figure 4-5. Flow pattern of a radial-flow turbine in a baffled column with draft tube. (Redrawn from McCabe et al, Unit operation of chemical engineering. 1993, p.392)

4.4 Design Parameters

In principle, the design and fabricate the gas-liquid-solid fluidized bed were necessary to estimate these design parameters as terminal velocity, minimum porosity, the height of bed at minimum fluidization, and minimum fluidization velocity. The equation for these parameters estimation and the standard turbine design would be stated in this section.

4.4.1 Terminal velocity, u_t

Terminal velocity of a single particle could be considered with an assumption that the particle moving through a fluid under the action of an external force. If the external force was the acceleration of gravity, g, which was constant. Also, the drag force always became larger with an increasing in velocity. The particle quickly reached a constant velocity, which was the maximum attainable under the circumstances, and which was called the terminal velocity. The equation for the terminal velocity was

$$u_t = \sqrt{\frac{2g(\rho_p - \rho)m}{A_p \rho_p C_D \rho}} \qquad (4\text{-}4)$$

where g = acceleration of gravity (m/s^2)

ρ_s = density of particle (kg/m^3)

ρ = density of fluid (kg/m^3)

m = mass of particle (kg)

A_p = projected were of particle measured in plane perpendicular to direction of motion of particle (-)

C_D = drag coefficient (-)

If the particles were spheres of diameter, D_p,

$$m = \frac{1}{6}\pi D_p^3 \rho_p \qquad (4\text{-}5)$$

and

$$A_p = \frac{1}{4}\pi D_p^2 \qquad (4\text{-}6)$$

Substitution of m and A_p, the terminal velocity became

$$u_t = \sqrt{\frac{4g(\rho_p - \rho)D_p}{3C_D \rho}} \qquad (4\text{-}7)$$

In general case, the terminal velocity could be found by trial and error after guessing Reynolds number, $N_{re,p}$ to got an initial estimate of drag coefficient, C_D, which the relation between Reynolds number and drag coefficient was shown in Figure 4-6.

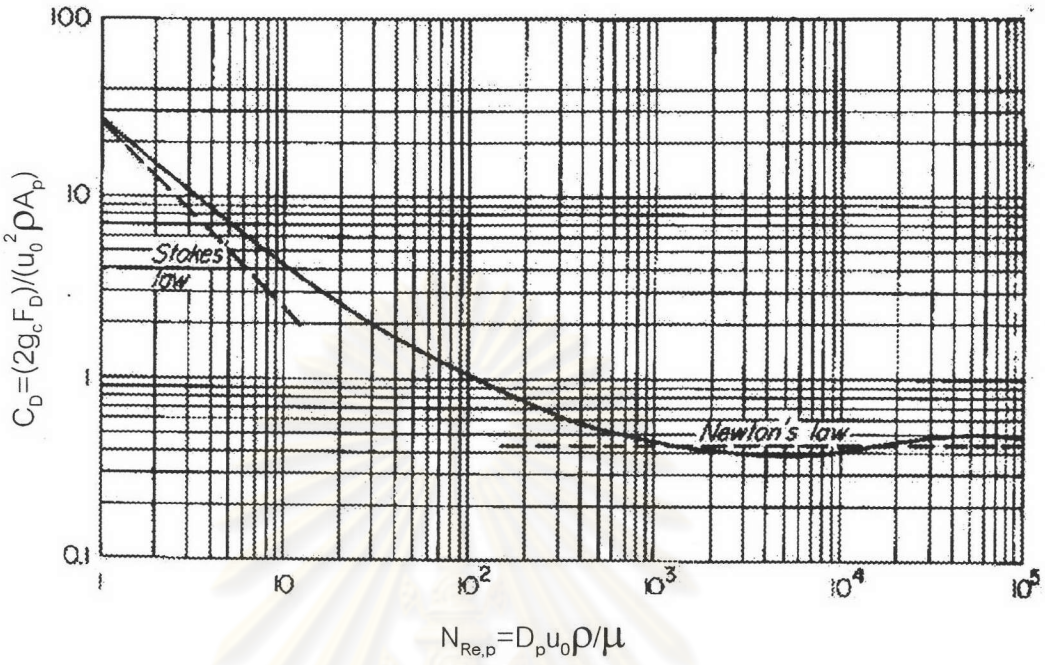

Figure 4-6. The relation between Reynolds number and Drag coefficient (Redrawn from McCabe et al, Unit operation of chemical engineering. 1993, p.158)

4.4.2. Minimum porosity, ε_{mf} and the height of bed at minimum fluidization

The minimum porosity was the minimum voidage, which could be determined by passing the fluid up through the bed, and noting the bed height at incipient particle notion or minimum fluidization. The correlation between the minimum porosity and the height of bed at minimum fluidization was

$$\varepsilon_{mf} = 1 - \frac{W}{L_{mf} A(\rho_p - \rho)} = \frac{L_{mf} - L}{L_{mf}} = 1 - \frac{L_0}{L_{mf}} \qquad (4\text{-}8)$$

where W = weight of solids in the bed

L_0 = height of bed at fixed bed

L_{mf} = height of bed at minimum fluidization

A = cross section area of column.

Fixed bed systems were low mixing, yield small axial dispersion of phases and so on, so fluidization was importance in many application. Therefore minimum porosity was significance to find minimum fluidization velocity.

4.4.3. Minimum fluidization velocity, u_{mf}

Minimum fluidization velocity was the velocity of fluid, which the solid particles moved apart and few vibrate. The equation for minimum fluidization velocity (would known as Ergun equation) was

$$\frac{150\mu u_{mf}}{\phi_s^2 D_p^2}\frac{(1-\varepsilon_{mf})}{\varepsilon_{mf}^3}+\frac{1.75\rho u_{mf}^2}{\phi_s D_p}\frac{1}{\varepsilon_{mf}^3}=g(\rho_p-\rho) \qquad (4\text{-}9)$$

where μ = fluid viscosity (kg/ m.s)

ε_{mf} = minimum porosity (-)

ϕ_s = sphericity (-)

If ε_{mf} and the physical properties of fluid and solid particle were given, u_{mf} could determine by equation (4-9). However, for very small particles, only the laminar flow term of Ergun equation was significant. With $N_{re,\,p} < 1$, the equation for minimum fluidization velocity became

$$u_{mf}=\frac{g(\rho_p-\rho)}{150\mu}\frac{\varepsilon_{mf}^3}{1-\varepsilon_{mf}}\phi_s^2 D_p^2 \qquad (4\text{-}10)$$

Many empirical equations state that u_{mf} varied with somewhat less than the 2.0 power of the particle size and not quite inversely with the viscosity. Slight deviations from the expected exponents occurred because there was some error in neglecting the second tern of Ergun equation and because the void fraction ε_{mf} might change with particle size. For roughly spherical particles, ε_{mf} generally laid between 0.40 and 0.45, and increases slightly with decreasing particle diameter. For irregular solids, the

uncertainty in ε_{mf} was probably the major error in prediction of u_{mf}. Usually, equation (4-10) was applied for particle about 30 -300 μm in size.

However, fluidization was also used for particles larger than 1 mm, as in the fluidized bed combustion of coal. In the limit of very large sizes, the laminar flow term became negligible, and u_{mf} varied with the square root of the particle size. The equation for $N_{re.P} > 10^3$ was

$$u_{mf} = \left[\frac{\phi_s D_p g(\rho_p - \rho)\varepsilon_{mf}^3}{1.75\rho} \right]^{1/2} \qquad (4\text{-}11)$$

4.4.4. Standard turbine design

A turbine agitator of the type shown in Figure 4-7 was commonly used. Typical proportions were

$D_a/D_t = 1/3$	$H/D_t = 1$	$J/D_t = 1/12$
$E/D_t = 1/3$	$W/D_a = 1/5$	$L/D_a = 1/4$

where D_a = diameter of agitator

D_t = diameter of tank

E = height of agitator above the column floor

H = depth of liquid in column

J = width of baffles

L = length of agitator blades

W = agitator width

The listed "standard" proportions were widely accepted and were the basis of many published correlation of agitator performance.

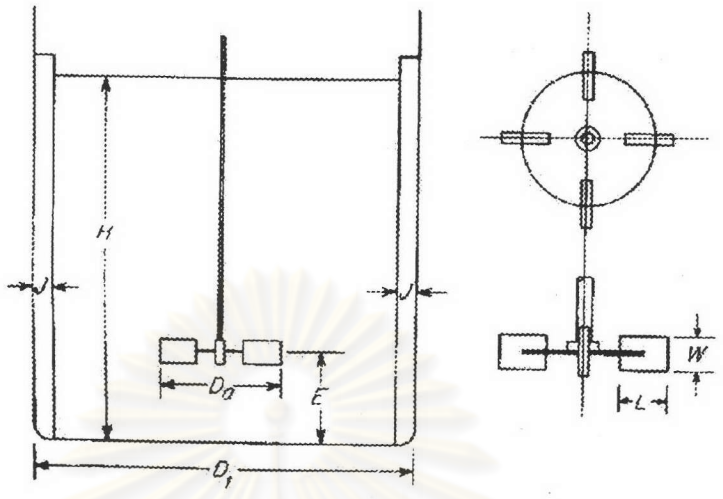

Figure 4-7. Measurement of turbine

(Redrawn from McCabe et al, Unit operation of chemical engineering. 1993, p.158)